Beam-Induced Multipactoring and Electron-Cloud Effects in Particle Accelerators

Fritz Caspers[(1)], Giovanni Rumolo[(1)], Walter Scandale[(1)], Frank Zimmermann[(1)]

[(1)]*CERN, 1211 Geneva 23, Switzerland*
Email: fritz.caspers@cern.ch ; giovanni.rumolo@cern.ch ; walter.scandale@cern.ch ; frank.zimmermann@cern.ch

INTRODUCTION

High-energy particle accelerators produce intense charged particle beams, e.g. of electrons or protons, at multi-GeV or multi-TeV energies, either shooting a single such beam against a fixed target or colliding two beams, in order to produce new particles and to study the scattering events in the search for the fundamental laws of physics.
In the beam pipe of these accelerators an "electron cloud" can be generated by a variety of processes, e.g. by residual-gas ionization, by photoemission from synchrotron radiation, and, most importantly, by secondary emission via a "beam-induced multipactoring" process [1]. The electron accumulation is most pronounced for positively charged particle beams, consisting e.g. of positrons or protons. The electron cloud causes a number of undesirable effects: It commonly leads to a degradation of the beam vacuum by several orders of magnitude [1-2], to fast beam "instabilities" [3-7], to beam size increases, as well as to fast or slow beam losses [3-8]. Since more than 40 years, electron-cloud effects of various flavors have been observed with particle beams. They have often limited the ultimate accelerator performance.
The electron cloud is a concern for the new 27-km 14-TeV Large Hadron Collider (LHC), soon to start operation at the European Organization for Nuclear Research, CERN, whose accelerator complex is shown in Fig. 1. Several electron-cloud effects are already being observed with LHC-type beam in the lower-energy LHC injectors, especially in the Super Proton Synchrotron (SPS) and the Proton Synchrotron (PS). At the new machine, the LHC proper, the cloud electrons can also give rise to a heat load inside the cold superconducting magnets [9-10] which, if exceeding the limited cooling capacity at cryogenic temperature, could lead to the magnets' transition into the normal-conducting state ("quench"). In addition to the direct heat deposition from incoherently moving electrons, the possibility of a "magnetron effect" has also been conjectured, where electrons would radiate coherently when moving in a strong magnetic field under the simultaneous influence of a beam-induced electric "wake" field that might become resonant with the cyclotron frequency.
In particle accelerators, there is another similar, but more violent, class of processes involving secondary electron emission and electron amplification, namely the multipactoring and breakdown phenomena which limit the accelerating gradient in normal- or super-conducting radiofrequency (rf) cavities used for beam acceleration and for longitudinal focusing. These rf-induced processes can lead to a "trip" of the affected rf cavity, normally resulting in immediate beam loss. Many of the cures initially developed to combat electron multipacting and breakdown in rf cavities, like surface coating with TiN [11], fine surface grooves [12], solenoidal magnetic fields [13], injection of uncorrelated microwaves [14], or ~kV dc electric bias fields at the rf couplers [14], have also proven effective against the beam-induced electron cloud.

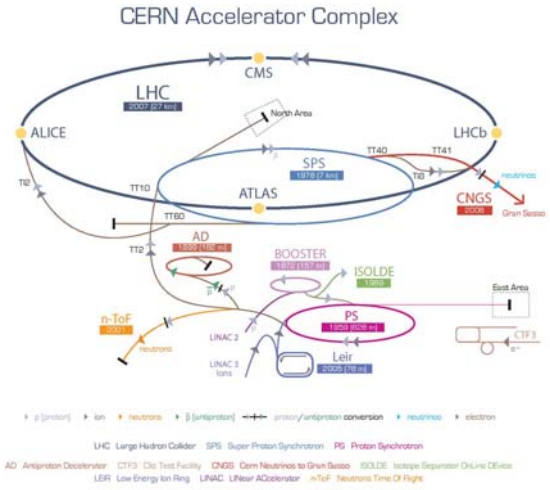

Fig. 1. The CERN accelerator complex including the Large Hadron Collider (LHC).

ELECTRON CLOUD IN ACCELERATORS

Since the 1960's effects related to electrons have been observed in accelerators of positively charged beams. The performance of almost all presently operating high-current positron and proton accelerators is affected by an electron cloud [6], which is generated by photoemission when synchrotron-radiation photons hit the surface of the beam pipe, by the ionization of the residual gas, and by an avalanche process involving acceleration of electrons in the field of the beam together with an average secondary emission yield larger than unity, as is illustrated for nominal LHC conditions in Fig. 2. Different from the multipactoring in rf cavities, the electron cloud or "beam-induced" multipactoring occurs without a sharp resonance for a wide range of bunch spacings and bunch intensities. The reason is that the low-energy secondary electrons have a long survival time, and therefore the exact arrival time of the next bunch is not important.

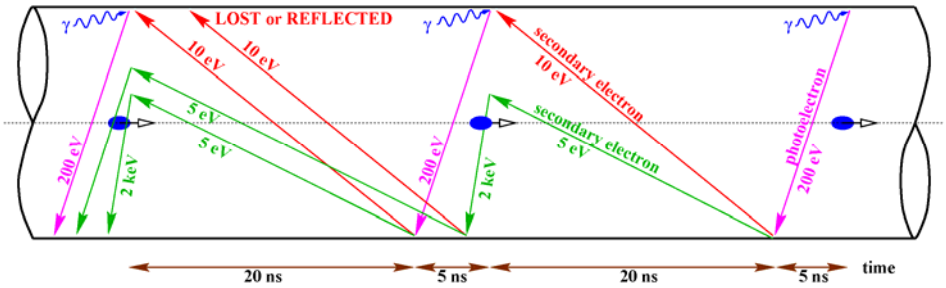

Fig. 2. Schematic of electron cloud build up in an LHC arc beam pipe, due to photoemission and secondary emission [F. Ruggiero]

KEY SURFACE PROPERTIES

Critical surface parameters for the electron-cloud build up, in particular the photo-emission yield [15] and secondary yield [16-19] under various conditions (e.g. rough surfaces, coatings, after electron bombardment, in magnetic fields, at cryogenic temperatures, with different angles of incidence), have been measured in laboratory set ups as well as in test beam lines at CERN and at BINP in Sibiria. An example shown in Fig. 3 indicates that the probability of elastic electron reflection might approach a value close to 1 for zero incident energy, independently of the maximum secondary emission yield. Benchmarking of computer simulations against beam measurements at the SPS suggests, however, that the reflection probability approaches a value of about 0.3, for the SPS warm stainless steel beam pipe [19], possibly in line with [18].

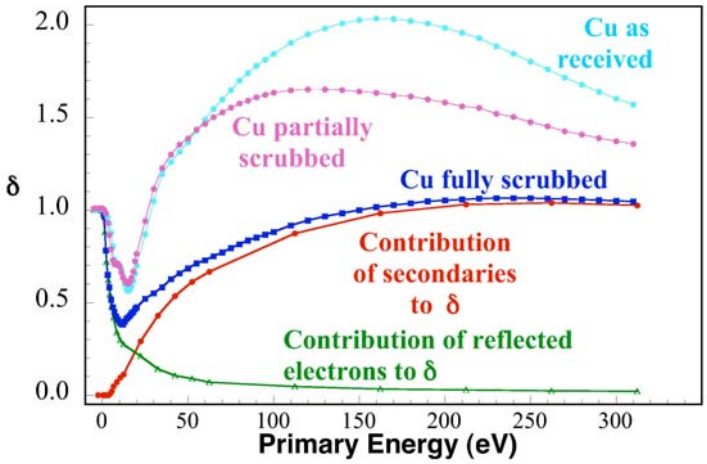

Fig. 3. Secondary emission yield δ for perpendicular incidence measured for a Cu surface at 10 K in various states of conditioning, and contributions of secondary and reflected electrons after full "scrubbing," as a function of primary electron energy [19].

ELECTRON-CLOUD DIAGNOSTICS AND OBSERVATIONS

Experiments with LHC type beam in the CERN Super Proton Synchrotron (SPS) and Proton Synchrotron (PS), which serve as LHC injector and pre-injector, respectively, have shown a rapid buildup, over about 40 bunches corresponding to 1 microsecond, of an electron cloud by beam-induced multipactoring, even without any synchrotron radiation for the SPS injection beam energy of 26 GeV. At the nominal LHC bunch spacing of 25 ns, the multipacting is observed for bunch populations above $3x10^{10}$ protons per bunch at the start of a run. Simulations confirm that it may be triggered by a small number of electrons generated by the beam ionization of the residual gas. The intensity threshold increases to 10^{11} protons per bunch after 10 days of 'scrubbing' (continuous operation with LHC beam at the maximum possible intensity and duty cycle permitted by electron-induced pressure rise). In the SPS the two main effects of the electron cloud are a pressure increase by several orders of magnitude [2] and beam instabilities that can lead to emittance growth and even beam loss (coupled bunch instability in the horizontal plane and single-bunch instability in the vertical plane) [21,22]. Degradation of BPM signals or feedback pick-ups due to electron bombardment were also observed; these could be partially cured by solenoid windings or by processing the data at higher frequencies (the electron-cloud build up over 100s of ns is a lower frequency phenomenon compared with the 0.5 ns rms bunch length) [23].
Since about 2000, a large number of detectors have been installed in the SPS to benchmark the electron-cloud simulations and to explore possible countermeasures. Some of these detectors are presented in Fig. 4 [24]. Promising results were achieved. In particular, vacuum chambers coated with TiZrV getter material [25] showed no sign of multipactoring, which suggests that the solution adopted for the warm parts of the LHC, about 10% of the circumference, will work fine. Also a fast surface conditioning by scrubbing was demonstrated in the SPS arcs. After 1 or 2 weeks of scrubbing the electron cloud did no longer limit the SPS operation with LHC beam. In situ measurements confirmed a considerable reduction of the maximum secondary emission yield, decreasing from about 2.0 to 1.5 over the same time period. However, measurements with two cold chambers in the SPS have shown a much slower scrubbing; see, e.g., [26]. This could be due to the fact that the cold sections were too short and influenced by gas influx from the adjacent warm vacuum chambers. A large number of gas molecules cryosorbed on the cold surface could lead to an enhanced secondary emission yield. In the laboratory, cold surfaces did show a conditioning similar to that of warm samples [19].

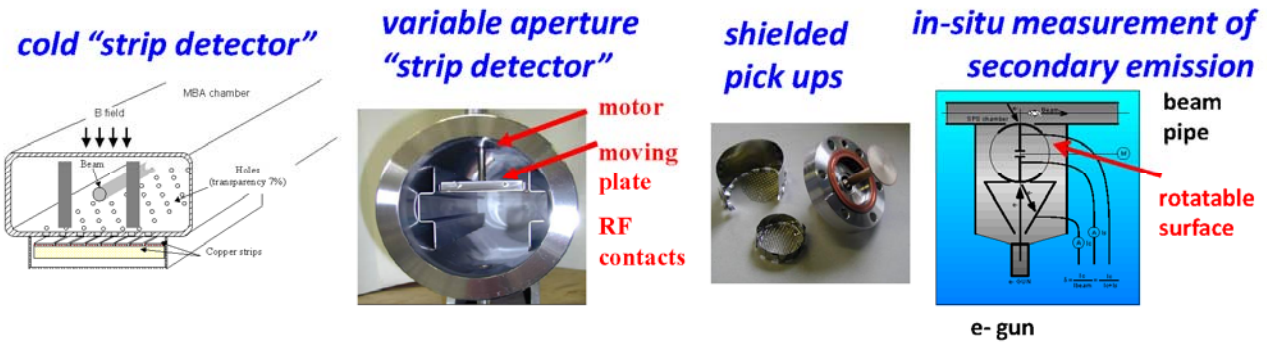

Fig. 4. Example electron-cloud diagnostics in the CERN SPS [24].

MICROWAVE TRANSMISSION MEASUREMENTS AND MAGNETRON EFFECT

Microwave transmission measurements represent a novel type of diagnostics which is sensitive to the average electron density over a long section of an accelerator. The underlying idea is that when electromagnetic waves are transmitted through a not too dense electron plasma, they experience a phase shift plus, possibly, a small attenuation. The phase shift expected for propagation through a uniform electron cloud of density ρ_e in free space, after a distance L, is

$$\Delta\phi = -1/2\,\omega_p^2 / (\omega_{rf} c) L$$

where ω_{rf} denotes the angular microwave rf frequency and ω_p the plasma frequency, $\omega_p \equiv \sqrt{4\pi\rho_e r_e c^2}$, with r_e representing the classical electron radius and c the speed of light. Assuming a typical electron density of 10^{12} m^{-3}, at microwave frequencies between 2 and 3 GHz the expected phase shift over 1 km is of order -20°. In the ionosphere, wheree the maximum ion density is comparable to the usual electron cloud density in accelerators, the corresponding phase shift limits the accuracy of the Global Positioning System (GPS) [27]. Over 500 km of propagation through the ionosphere, the measured phase delay is or order 1 m, or equivalently 4 degrees per km.

If the electrons are not in free space but inside a beam pipe with cutoff frequency ω_c, the phase shift becomes [28,29]

$$\Delta\phi = -1/2\,\omega_p^2 \Big/ \left(\sqrt{\omega_{rf}^2 - \omega_c^2}\,c\right) L\,.$$

In the presence of a static magnetic field of strength B perpendicular to the beam pipe and to the propagation direction of the microwaves, an enhancement proportional to $1/\left(1-\left(eB/\left(\omega_{rf}\,m_e\right)\right)^2\right)$ is expected near the cyclotron resonance.

The left picture of Fig. 5. shows a microwave transmission measurement in the Low Energy positron Ring of the "PEP-II B Factory" at the Stanford Linear Accelerator Center [28]. In this ring, the electron cloud build up is normally suppressed by a weak solenoid field o about 20 G generated by current-carrying wires wrapped around the beam pipe. If the solenoids are turned off, an electron cloud develops, which leads to a phase modulation of the transmitted signal that is evident by the appearance of sidebands, separated from the carrier frequency by multiples of the 136 kHz revolution frequency. The modulation signal appears since the electron cloud first builds up and then decays to zero in a long "clearing gap" without bunches, on each revolution period. The electron cloud density can be inferred from the amplitude of the sideband with respect to the carrier. The right picture shows evidence for a cyclotron resonance in similar measurements at another accelerator [30].

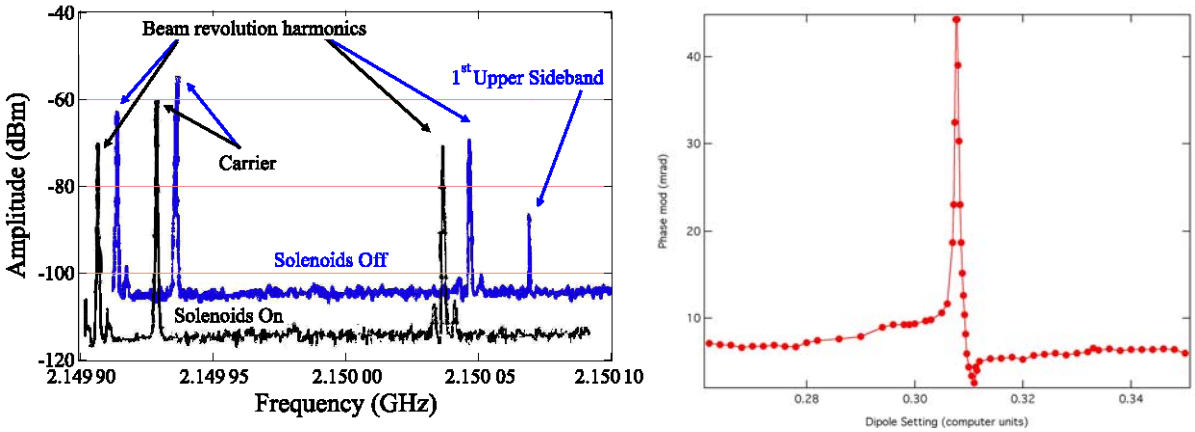

Fig. 5. Left: Spectrum analyzer traces showing microwave carrier and beam signals measured in the PEP-II Low Energy Ring over a distance of 50 m with a carrier at 2.15 GHz. A phase modulation sideband appears when the solenoid fields of 20 G covering the entire region is turned off, allowing the electron plasma to fill the beam pipe. Only the upper sideband is shown [28]. Right: Microwave phase modulation amplitude measured over a length of 4 m in the CESR-TA accelerator with a carrier frequency of 2.015 GHz. The dipole setting at the peak of about 0.307 units corresponds to a field of 700 T and to a cyclotron resonance near 2 GHz [30].

With short positron bunches passing through a magnetic dipole field, resonances in the cloud build up have been seen when the bunch spacing equals a multiple of the cyclotron period [31] and reproduced in simulations [32]. During a bunch passage the electrons are subjected to a strong transverse electric field. In a dipole field, the cyclotron frequency equals 28 GHz/Tesla multiplied with the field strength. At the LHC, the proton bunch length itself extends over many cyclotron periods, so that a sharp resonance between the cyclotron motion and the bunch spacing is not probable. However, another resonance effect is possible. If the geometry of the LHC beam pipe allows for some beam-excited trapped modes at suitable frequencies (indeed, due to the fabrication process there are minor mechanical undulations in the beam tube), at a certain value of the magnetic field, during the beam acceleration, one might encounter an accidental "magnetron effect" where the frequency of the trapped modes matches the cyclotron frequency of cloud electrons. This would give rise to a (local) coherent emission at the cyclotron frequency, which could occur at any value between 15 GHz and 230 GHz depending on the B field. The 1-mm deep, 1.5-mm wide, and 8-mm long rectangular pumping slots (500 per meter) in the LHC beam pipe, at 5-20 K temperature, will only shield radiation up to about 15 GHz. At higher frequencies, any RF radiation can pass onto the cold bore of the magnets. The bunch potential would act as intermittent anode voltage of this device. The possibility of such magnetron effect in the LHC was first thought of when in early laboratory measurements using a resonant coaxial structure a substantial decrease of the multipactoring threshold was observed for an external dipole magnetic field (170 Gauss) such that the electron cyclotron frequency was equal to the resonant frequency of the coaxial cavity (480 MHz) [33]. The dip visible in Fig. 6 was caused by the resulting cavity impedance mismatch, related to the refraction index of the electron plasma, leading to a large reflected signal.

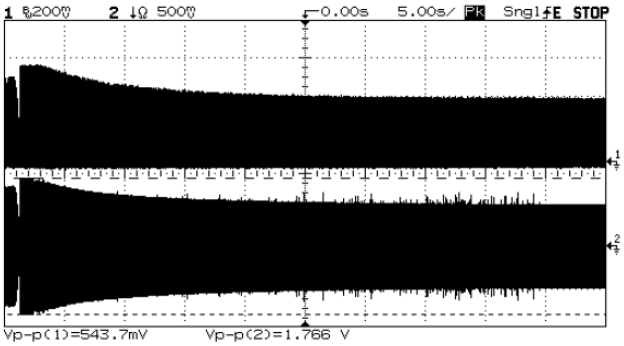

Fig. 6. Multipactoring tests in a warm dipole magnet: deposited power (top, 2.5 W peak) and transmitted signal (bottom) measured during a 50 s ramp of the dipole field from 100 up to 7800 Gauss. The dip on the left corresponds to a magnetic field of 170 Gauss, when the cyclotron frequency of the electrons becomes equal to the RF frequency of 480 MHz. AM modulation frequency 20 Hz, DC-bias 100 V, RF forward power 4 W [33].

ELECTRON-CLOUD MITIGATION

The LHC design has adopted a number of countermeasures against the electron cloud. For example, most vacuum chambers in the warm sections of the LHC are coated by a newly developed getter material, TiZrV [25], which after activation for 24 h at 180 ^{o}C has a low maximum secondary emission yield δ_{max} of about 1.1. Other coatings, e.g. ones based on carbon composites or rough metal surfaces, are under exploration for the LHC injector upgrade [34]. In the LHC cold arcs, a sawtooth pattern (steps of 35 micron separated by 500 micron) is impressed on the horizontally outward side of the beam screen that forms the inner layer of the vacuum chamber [15]. The sawtooth pattern results in a locally perpendicular impact of synchrotron-radiation photons yielding both a strongly reduced reflectivity and a lower photoemission yield. The reduced reflectivity is important as, in dipole magnets, photoelectrons emitted at the outer side of the chamber are confined and do little harm to the beam, while photoelectrons emitted at the top and bottom of the chamber, via scattered photons, may approach the beam and contribute to multipactoring and heat load.
The LHC beam screen contains pumping slots at its top and bottom. Multipactoring electrons which pass through these slots along the magnetic field lines would hit the cold bore of the magnets at 2 K, where the available cooling capacity is much smaller than at the beam-screen temperature of 5-20 K. To prevent this fatal heat load, pumping-slot shields ('baffles') were added on the outer side of the beam screen, so as to intercept such electrons, at the expense of a slightly reduced pumping speed [35,36].
Heat load on the beam screen and vacuum pressure can be confined to tolerable values, by reducing either the number of bunches or the bunch charge. For a three times increased bunch spacing of 75 ns, no significant heat load from the electron cloud is expected. Alternatively, bunch populations below $5x10^{10}$ at the nominal bunch spacing of 25 ns may also yield an acceptable heat load. In addition, low-charge 'satellite' bunches, following 5 or 10 ns behind the main bunches, could be employed as a fall back option to suppress the electron-cloud build up and to reduce the heat load during commissioning [37].
The surface of the LHC vacuum chamber will be conditioned by operating near the heat-load limit for extended periods of time (the 'scrubbing' effect is described in [16]). At the LHC this 'scrubbing' will be more difficult than in the SPS, since the electron cloud activity will increase during acceleration, due to additional contributions from synchrotron radiation and the reduced beam sizes. It is expected, that after several weeks or months of operation, the surface conditioning during commissioning and early operation will reduce the secondary emission yield to a level where operation with nominal LHC beam parameters becomes possible.
Measurements in the SPS have highlighted the extreme sensitivity of the electron-cloud build up to the chamber surface and its secondary emission yield. Recently the total electron-cloud flux at the chamber wall for fully activated TiZrV NEG coating, with a maximum secondary yield δ_{max}~1.1, was found to be 10^{-4} times smaller than that for an otherwise identical stainless steel chamber, with a measured maximum yield of δ_{max}~2.5 after 2-h air exposure; the flux recorded for a carbon surface with δ_{max}~1.4 after a similar 2-h air exposure was 4 times smaller than for the stainless steel chamber; a clear scrubbing effect was observed for both the carbon and the steel [38].
Other suppression schemes are also being explored in the LHC injectors. Fig. 7 shows the electron-cloud signal from a pick up in the PS as a function of dipole magnetic field and "strip-line" clearing voltage applied in the region of the detector, for two different times in the PS acceleration cycle, differing in longitudinal beam profile and bunch length

[39]. The dependence of the electron-cloud density on the two mitigation parameters is complex, with islands of high electron density, indicating multipactoring, embedded in large regions with only few electrons.

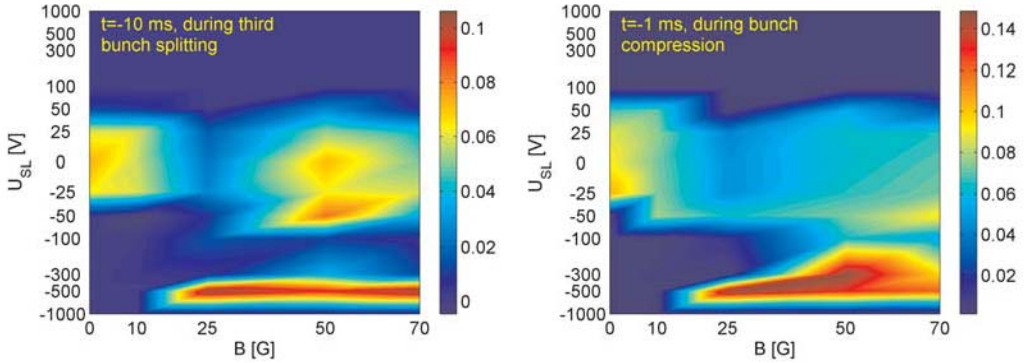

Fig. 7. Electron cloud signal at the CERN PS in units of Volt measured for various clearing electrode voltages (-1 kV < U_{SL} < +1 kV) and magnetic dipole fields (0 G < B < 70 G). Measurements were taken continuously during the last 50 ms before beam extraction at t = 0 ms [39].

SIMULATIONS

Several simulation codes modelling electron-cloud build up and/or the beam instabilities driven by an electron cloud have been developed since the mid 1990s; a code overview can be found in [40]. The crucial ingredient for the build-up simulations is the model of the "total" secondary emission yield δ_{tot}, consisting of both true secondaries and reflected (plus re-diffused) electrons, which is a function of the primary electron energy E_p and the angle of incidence θ (θ=0 refers to perpendicular impact). For LHC simulations with the codes ECLOUD or Faktor2 we use

$$\delta_{tot}\left(E_p,\theta\right)=\delta_{true}\left(E_p,\theta\right)+R\delta_{elastic}\left(E_p\right)$$

with reflection coefficient R~0.3 extracted from beam measurements [13]. The true secondary yield is taken to be [41]

$$\delta_{true}\left(E_p,\theta\right)=\delta_{\max}\left(\theta\right)\frac{s\times\left(E_p/E_{\max}\left(\theta\right)\right)}{s-1+\left(E_p/E_{\max}\left(\theta\right)\right)^s}$$

where maximum yield δ_{max} and primary energy of maximum yield, E_{max}, depend on the angle of incidence as [17,18,42]

$$\delta_{\max}\left(\theta\right)\approx\delta^*_{\max}\exp\left(\frac{1}{2}\left(1-\cos\theta\right)\right)$$

$$E_{\max}\left(\theta\right)\approx E^*_{\max}\times\left(1+0.7\left(1-\cos\theta\right)\right)$$

with typical measured values for copper of δ^*_{max} ~ 1.5 and E^*_{max} ~ 240 eV after two days of beam scrubbing, as was inferred from in-situ measurements at the SPS [42]. The elastic contribution is parametrized as

$$\delta_{elastic}\left(E\right)\approx\left(\frac{\sqrt{E}-\sqrt{E+E_0}}{\sqrt{E}+\sqrt{E+E_0}}\right)^2$$

with E_0~150 eV fitting the data well [19]. For reliable predictions, it is important to benchmark the simulation results from different codes with each other as well as against laboratory measurements or beam observations [20,33,43,44].

OPEN QUESTIONS

The simulated heat load strongly depends on the reflection probability of low-energetic electrons when they hit the chamber wall. This reflectivity has a great influence on the survival of secondary electrons between bunches and, in particular, during the gaps between bunch trains.

A strong increase in the gas pressure during LHC scrubbing would reduce the beam lifetime and increase the heat load on the cold bore of the magnets due to scattered proton losses. This source of heat load may complicate the scrubbing process with respect to the SPS, in addition to a reduced duty cycle and to the new effects of synchrotron radiation and photoemission encountered in the LHC towards top energy. A related concern is that low energy electrons hitting the wall, if there are many, could amount to a significant heat load, without contributing to surface conditioning [45]. For the latter a minimum electron energy of about 30 eV is required [46].

SUMMARY

Electron-cloud build up can affect the operation of particle accelerators. The electron build up sensitively depends on the surface properties and in particular on the secondary emission yield. Special diagnostics tools have been developed which measure the local or global electron density, the spatial distribution, the time structure, the flux of electrons incident on a surface, the electron energy distribution, the heat deposition from electrons, or the surface conditioning. A large number of methods have been applied to suppress electron cloud build-up, including various coatings with low secondary emission yield, fine grooves, ~kV dc clearing voltages, and weak magnetic fields tangential to the surface.

ACKNOWLEDGEMENTS

The contents of this presentation is the result of the work of many people, at CERN and around the world, including Gianluigi Arduini, Vincent Baglin, Giulia Bellodi, Elena Benedetto, Oliver Bruning, Paolo Chiggiato, Roberto Cimino, Ian Collins, Giuliano Franchetti, Hitoshi Fukuma, Miguel Furman, Oswald Grobner, Sam Heifets, Noel Hilleret, Bernard Jeanneret, Miguel Jimenez, Tom Kroyer, Jean-Michel Laurent, Edgar Mahner, Kazuhito Ohmi, Mauro Pivi, Francesco Ruggiero, Daniel Schulte, Elena Shaposhnikova, Mauro Taborelli, Laurent Tavian, Lanfa Wang, Jie Wei, and Xiaolong Zhang. We acknowledge the support of the European Community-Research Infrastructure Activity under the FP6 "Structuring the European Research Area" programme (CARE, contract number RII3-CT-2003-506395).

REFERENCES

[1] O. Grobner, "Bunch Induced Multipactoring," *Proc. Xth International Conference On High Energy Accelerators*, Vol. 2, Serpukhov 1977, pp. 277-282, 1977.

[2] J.M. Jimenez, G. Arduini, P. Collier, G. Ferioli, B. Henrist, N. Hilleret, L. Jensen, K. Weiss, F. Zimmermann, "Electron cloud with LHC-type beams in the SPS: A review of three years of measurements," *Proc. Mini Workshop on Electron Cloud Simulations for Proton and Positron Beams (ECLOUD'02)*, Geneva, Switzerland, 15-18 Apr 2002, pp. 17-18, CERN Yellow Report CERN-2002-001, 2002.

[3] K. Ohmi, "Beam-Photoelectron Interactions in Positron Storage Rings," *Phys. Rev. Lett.* 75, 1526, 1995.

[4] K. Ohmi and F. Zimmermann, "Head-Tail Instability Caused by Electron Clouds in Positron Storage Rings," *Phys. Rev. Lett.* 85, 3821, 2000.

[5] K. Ohmi, F. Zimmermann, and E. Perevedentsev, Wake-field and fast head-tail instability caused by an electron cloud," *Phys. Rev. E* 65, 016502, 2002.

[6] F. Zimmermann, "Review of single bunch instabilities driven by an electron cloud," *PRST-AB* 7, 124801, 2004.

[7] G. Rumolo and F. Zimmernann, "Electron cloud simulations: beam instabilities and wakefields," *Phys. Rev. ST Accel. Beams* 5, 121002, 2002.

[8] E. Benedetto, G. Franchetti, and F. Zimmermann, "Incoherent Effects of Electron Clouds in Proton Storage Rings," *Phys. Rev. Lett.* 97, 034801, 2006.

[9] O. Bruning, "Simulations for the beam induced electron cloud in the LHC beam screen with magnetic field and image charges,"*CERN-LHC-PROJECT-REPORT*-158, Nov 1997. 2

[10] G. Rumolo, F. Ruggiero, and F. Zimmermann, „Simulation of the electron-cloud build up and its consequences on heat load, beam stability, and diagnostics," *Phys. Rev. ST Accel. Beams* 4, 012801, 2001.

[11] M. Kuchnir and E. Hahn, "Coating Power RF Components with TiN," *FNAL Internal Report, TM-1928* (1995); http://lss.fnal.gov/archive/test-tm/1000/fermilab-tm-1928.shtml

[12] T. Abe, T. Kageyama, H. Sakai, Y. Takeuchi, "Fine Grooving of Conductor Surfaces of RF Input Coupler to Suppress Multipacting," *Prof. 10th European Particle Accelerator Conf. (EPAC'06)*, Edinburgh, p. 1310, 2006.

[13] D.C. Nguyen et al (17 authors), "Initial Performance of Los Alamos Advanced Free Electron Laser," *Proc. 15th International Free Electron Laser Conference*, The Hague, Netherlands, 23-27 August, 1993.

[14] J. Tückmantel, C. Benvenuti, D. Bloess, D. Boussard, G. Geschonke, E. Haebel, et al (12 authors), "Improvements to Power Couplers for the LEP2 Superconducting Cavities," *Proc. 1995 Particle Accelerator Conference and International Conference on High Energy Accelerators (PAC9),* Dallas, p. 1642, 1995.

[15] V. Baglin, I.R. Collins, O. Grobner, "Photoelectron yield and photon reflectivity from candidate LHC vacuum chamber materials with implications to the vacuum chamber design,", *Proc. 6th European Particle Accelerator Conference (EPAC 98)*, Stockholm, Sweden, 22-26 June 1998, pp. 2169-2171, 1998.

[16] V. Baglin, Yu. Bozhko, O. Grobner, B. Henrist, N. Hilleret, C. Scheuerlein, M. Taborelli, "The secondary electron yield of technical materials and its variation with surface treatments," *Proc. 7th European Particle Accelerator Conference (EPAC 2000)*, Vienna, Austria, 26-30 Jun 2000, pp. 217-22, 2000.

[17] R. Kirby, F. King, "Secondary electron emission yields from PEP-II accelerator materials," *NIM* A 469:1, 2001.

[18] B. Henrist, N. Hilleret, M. Jimenez, C. Scheuerlein, M. Taborelli, G. Vorlaufer., "Secondary electron emission data for the simulation of electron cloud," *Proc. Mini Workshop on Electron Cloud Simulations for Proton and Positron Beams (ECLOUD'02)*, Geneva, 15-18 April 2002, pp. 75-78, CERN Report CERN-2002-001, 2002.
[19] R. Cimino, I. R. Collins, M. A. Furman, M. Pivi, F. Ruggiero, G. Rumolo, and F. Zimmermann, "Can Low-Energy Electrons Affect High-Energy Physics Accelerators?," *Phys. Rev. Lett.* 93, 014801, 2004.
[20] D. Schulte, G. Arduini, V. Baglin, J.M. Jimenez, F. Zimmermann, "Electron cloud measurements in the SPS in 2004," *Proc. Particle Accelerator Conference (PAC 05)*, Knoxville, Tennessee, 16-20 May 2005, pp 1371, 2005.
[21] G. Arduini, W. Hofle, G. Rumolo, F. Zimmermann, "Transverse Behavior of the LHC Proton Beam in the SPS: An Update," *Proc. 2001 Particle Accelerator Conference (PAC2001)*, Chicago, 18-22 June, 2001.
[22] K. Cornelis, "The Electron Cloud Instability in the SPS," *Proc. Mini Workshop on Electron Cloud Simulations for Proton and Positron Beams (ECLOUD'02)*, Geneva, Switzerland, 15-18 Apr 2002, pp. 11-16, CERN Yellow Report CERN-2002-001, 2002.
[23] W. Hofle, "Progress with the SPS damper," *Proc. 11th Workshop on LEP Performance*, Chamonix, France, 15-19 January 2001. CERN-*SL-2001-003-DI*, pp. 117-124, 2001.
[24] J.M.Jimenez, "Electron Cloud and Vacuum Effects in the SPS," *31st Advanced ICFA Beam Dynamics Workshop on Electron-Cloud Effects (ECLOUD'04),* Napa, 19-23 April, 2004, http://icfa-ecloud04.web.cern.ch/icfa-ecloud04/agenda.html .
[25] C. Benvenuti P. Chiggiato, P. Costa Pinto, A. Escudeiro Santana, T. Hedley, A. Mongelluzzo, V. Ruzinov, I. Wevers, "Vacuum properties of TiZrV non-evaporable getter films," *Vacuum* 60, pp. 57-65, 2001.
[26] V. Baglin, I.R. Collins, B. Jenninger, "Performance of a cryogenic vacuum system (COLDEX) with a LHC type proton beam," *Vacuum* 73, pp. 201-206, 2004.
[27] T. Herring, "Modern Navigation," Lecture at MIT, Massachusetts, http://chandler.mit.edu/~tah/12.215 .
[28] S. De Santis, J. M. Byrd, F. Caspers, A. Krasnykh, T. Kroyer, M. T. Pivi, and K. G. Sonnad, "Measurement of Electron Clouds in Large Accelerators by Microwave Dispersion," *Phys. Rev. Lett.* 100, 094801, 2008.
[29] H. S. Uhm, K. T.Nguyen, R. F. Schneider, and J. R. Smith, "Wave dispersion theory in a plasma column bounded by a cylindrical waveguide," *J. Appl. Phys.* **64**, 1108, 1988.
[30] J. Byrd, M. Billing, S. De Santis, M. Palmer, J. Sikora, "Measuring Electron Cloud Density at CesrTA by Microwave Transmission," *ILC Damping Ring R&D Workshop 2008*, 8-11 July 2008, Cornell University, 2008.
[31] C.M. Celata, M. Furman, J.-L. Vay, J.W. Yu, "Electron Cyclotron Resonances in Electron Cloud Dynamics," Presented at *11th European Particle Accelerator Conf. (EPAC'08)*, Genoa, 23-27 June, 2008.
[32] M. Pivi et al (19 authors), "A New Chicane Experiment in PEP-II to Test Mitigations of the Electron Cloud Effect for Linear Colliders," *11th European Particle Accelerator Conf. (EPAC'08)*, Genoa, 23-27 June, 2008.
[33] O. Bruning, F. Caspers, J.M. Laurent, M. Morvillo, F. Ruggiero, "Multipacting tests with magnetic field for the LHC beam screen," *Proc. 6th European Particle Accelerator Conference (EPAC 98)*, Stockholm, Sweden, 22-26, 1998, pp. 356-358, 1998.
[34] P. Chiggiato, private communication, 2008.
[35] N. Kos, "Pumping Slot Shields for LHC Beam Screens," CERN *Vacuum Technical Note* 03-12 (2003).
[36] A. Krasnov, "Molecular pumping properties of the LHC arc beam pipe and effective secondary electron emission from Cu surface with artificial roughness," *Vacuum* 73, pp. 195-199, 2004.
[37] F. Ruggiero, X. Zhang, "Collective Instabilities in the LHC: Electron Cloud and Satellite Bunches," *Proc. Workshop on Instabilities of High Intensity Hadron Beams in Rings*, BNL, 28 June-1st July 1999, eds. T. Roser and S.Y. Zhang, *AIP Conf. Proceedings* 496, pp. 40-48, 1999.
[38] M. Taborelli, "Results from SPS run on e-cloud, coatings for low SEY," CERN APC meeting, 18 July 2008.
[39] E. Mahner, T. Kroyer, F. Caspers, "Electron cloud detection and characterization in the CERN Proton Synchrotron," accepted for publication in *PRST-AB*, 2008.
[40] CARE-HHH-APD Accelerator Physics Code Repository & Benchmarking Web Site http://oraweb.cern.ch:9000/pls/hhh/code_website.startup
[41] M.A. Furman, G.R. Lambertson, The electron-cloud instability in the arcs of the PEP-II positron ring," *Proc. International Workshpo on Multibunch Instabiltiies in Future Electron and Positron Accelerators (MBI97)*, Tsukuba, 15-18 July 1997, Ed. Y.H. Chin, KEK Proceedings 97-17, 1997.
[42] N. Hilleret, private communication, and "SEY and Pick-up Calorimeter Measurements," Mini-Workshop on 'SPS Scrubbing Run Results and Implications for the LHC', CERN, 28 June 2002, unpublished; see http://sl.web.cern.ch/SL/sli/Scrubbing-2002/Workshop.htm .
[43] F. Zimmermann, "Electron-Cloud Benchmarking and CARE-HHH Codes," *Proc. 39th ICFA Advanced Beam Dynamics Workshop on High Intensity High Brightness Hadron Beams 2006 (HB2006)*, Tsukuba, Japan, 29 May - 2 June 2006, pp. 350-352, 2006.
[44] M.A. Furman, V.H. Chaplin, "Update on electron-cloud power deposition for the Large Hadron Collider arc dipoles.," *Phys.Rev.ST Accel.Beams* 9:034403, 2006.
[45] V. Baglin, private communication, 2004.
[46] N. Hilleret, private communication, 2003.